General Disclaimer

One or more of the Following Statements may affect this Document

- This document has been reproduced from the best copy furnished by the organizational source. It is being released in the interest of making available as much information as possible.

- This document may contain data, which exceeds the sheet parameters. It was furnished in this condition by the organizational source and is the best copy available.

- This document may contain tone-on-tone or color graphs, charts and/or pictures, which have been reproduced in black and white.

- This document is paginated as submitted by the original source.

- Portions of this document are not fully legible due to the historical nature of some of the material. However, it is the best reproduction available from the original submission.

Produced by the NASA Center for Aerospace Information (CASI)

DOE/JPL 954902 - 79/4
Distribution Category UC - 63

(NASA-CR-162166) SILICON SOLAR CELL FABRICATION TECHNOLOGY Quarterly Report, 1 Jan. - 30 Apr. 1979 (California Univ.) 34 p HC A03/MF A01 CSCL 10A

N79-31755

Unclas G3/44 31877

FOURTH QUARTER REPORT TO J.P.L.

for period January 1 - April 30, 1979

Grant #954902

SILICON SOLAR CELL FABRICATION TECHNOLOGY

Published May 2, 1979

Principal Investigator: O. M. Stafsudd

U. C. L. A.

"The JPL Low-Cost Silicon Solar Array Project is sponsored by the U. S. Dept. of Energy and forms a part of the Solar Photovoltaic Conversion Program to initiate a major effort toward the development of low-cost systems.

"This report was prepared as an account of work sponsored by the United States Government. Neither the United States nor the United Stated Dept. of Energy, nor any of their employees nor any of their contractors, subcontractors, or their employees, makes any warranty, express or implied, or assumes any legal liability or responsibility for the accuracy, completeness or usefullness of any information, apparatus, product or process disclosed, or represents that its use would not infringe privately owned rights."

JPL Subcontractor Report

JPL FILE NO. 9950- 134

TITLE SILICON SOLAR CELL FABRICATION TECHNOLOGY

AUTHOR(S) O. M. Stafsudd

SUBCONTRACTOR U.C.L.A.

SUBCONTRACTOR REPORT NO. Fourth Quarterly Report

REPORT DATE May 2, 1979 PERIOD COVERED 1/1 - 4/30/79

JPL CONTRACT NO. 954902-79/4 PAGE COUNT

8/14/79kw

5 copies: 2-NASA, 2-Vellum, 1-Library

This document has been released for external distribution.

TECHNICAL SUMMARY

LASER SCANNER STUDIES:

During this quarter the laser cell scanner had been used to characterize a number of solar cells made in various materials. The cells were provided by J.P.L. and were identified as:

1.	RTR	850D-2	0.4	9.	Wacker Control	W-11-8	11.7
2.	RTR	868C4	1.7	10.	CSI	1-852-52	9.9
3.	WEB	RE 12-3.3.-2	9.8	11.	CSI	1-860-46	5.7
4.	WEB	J 65-3.4-10	8.9	12.	CSI	1-852-23	5.5
5.	WEB	RE 24-1.5-7 (BSF)	7.7	13.	CSI	1-852-41	9.9
6.	WACKER	W-11-3	8.7	14.	EFG	8	8.4
7.	WACKER	W-11-17	10.2	15.	EFG	28	10.3
8.	WACKER	W-4-4	10.6	16.	EFG	36	7.1

In the figures I-1 to 16-1 typical cell traces are shown. In each case the photo current is plotted horizontally, increasing current to the right, and the position of the illuminated spot is plotted vertically. The fingers of the collection grid show up as dips in the response curves. Each cell has at least two traces taken, one at 1/3 and a secomd at 2/3 the distance along the collection fingers. (See Fig. 1) These scans are performed with a Helium-Neon Laser @ .6328 microns wave length.

If the cells show any unusual features at .6388 microns further scans are run using the green and blue wave lengths of an argon ion laser. Because of the shorter wave lengths, the penetration depth is considerably less (1 micron as compared to 3 microns). The short wave length scans tend to show surface and shallow defects in cells. The longer wave length radiation

scans tend to show deep defects and or poor diffusion lengths.

To improve on capabilities in this area, we are going to provide .93 micron radiation for greater penetration depths in the near future in order to get more information with respect to diffusion length and the variation of diffusion length over a cell's surface.

Of particular interest is the RTR cell whose responses are shown in Figures II-1, 2, 3, 4. Figure II-1 and II-2 are scans across the finger pattern in the usual manner. It should be noted that these figures have current scales 10x smaller than typical cells such as Figure III-1. That is, the photo current is reduced by factors of 10 or more than typical cells. The photo current is seen to be a maximum near the fingers. This is quite unusual behavior and indicated extreme problems with the junction collection efficiency. The short wave length scan Figure 11-2 shows even more pronounced effect near the fingers.

Scans were run in perpendicular direction to the norm. That is, a scan was taken in the direction of the fingers. This is shown in Figure 11-3 the buss bar of the finger pattern is on the left and, as usual, current is plotted down (to the right of the page). In this case our normal current sensitivity is used. We see that the cell has a more or less normal current response near the buss bar and essentially dies suddenly as one precedes away from this area. The scan at the bottom of the Il-3 Figure is in the normal direction (across the fingers) but quite close to the buss bar. Again this scan is essentially the same as a normal cell. Therefore, the RTR cell which has a measured efficiency of 1.7% at AMI actually has only about 1/5 of the cell active. The active area of the cell actively has an efficiency of about 8.5%.

ELECTRON BEAM-INDUCED CURRENT STUDY:

The Cambridge "stereoscan" scanning electron microscope (type 96113 Mark 2A), suitably modified was used in our work. Faculties to take photographs and also record EBIC currents exist.

In our work planar p-n junctions were analyzed. A theory for the EBIC current based on the analytic solution of the ambipolar diffusion equation under the influence of electron beam excitation parameter z (which is related to beam penetration) the junction depth Z_j, the beam current and the surface recombination velocity s.

The theory was tested using a junction with differing junction depths and results agreed closely. Big 17 shows an EBIC picture of the shallow and deep parts of the device tested.

The effect of scribing was then examined. This caused the EBIC to dip almost to zero at the scribe. (See Fig. 18)

The effect of a grain boundary was then studied. The current dip was found to be much less drastic at the grain boundary than at the scribe. It was possible to estimate the effective diffusion length at the grain boundaries or rather put an upper limit on their values. We found that the ballooning effect of the beam as it penetrates the specimen was the limit in resolution. Hence, we determined that the "diffusion length" in the grain boundary region was less than 2 microns.

We therefrom estimated the equivalent grain boundary recombination velocity 5_{gb} to be in the region 1000 to 3000 Cm/s. The analysis was based on a piecewise linearization technique developed from the theory derived.

It was also recognized that humps in the current dip would be attributed to non-verticality of the grain boundary. (See Fig 19.)

A lot of scope for future work exists, primarily in the area of solving the 3-dimensionally ambipolar diffusion egn. near a grain boundary under electron beam excitation.

References: (1) Subramanian S. Lyn
Electron Beam Induced Current in a p-n Junction
Maniu Thesis UCLA (1978)

FINANCIAL

The total funds expended in this study up to March 31, 1979 is $35,448.38.

The students employed on this project were:

C. Davis, F. Choi and M. Ianglean

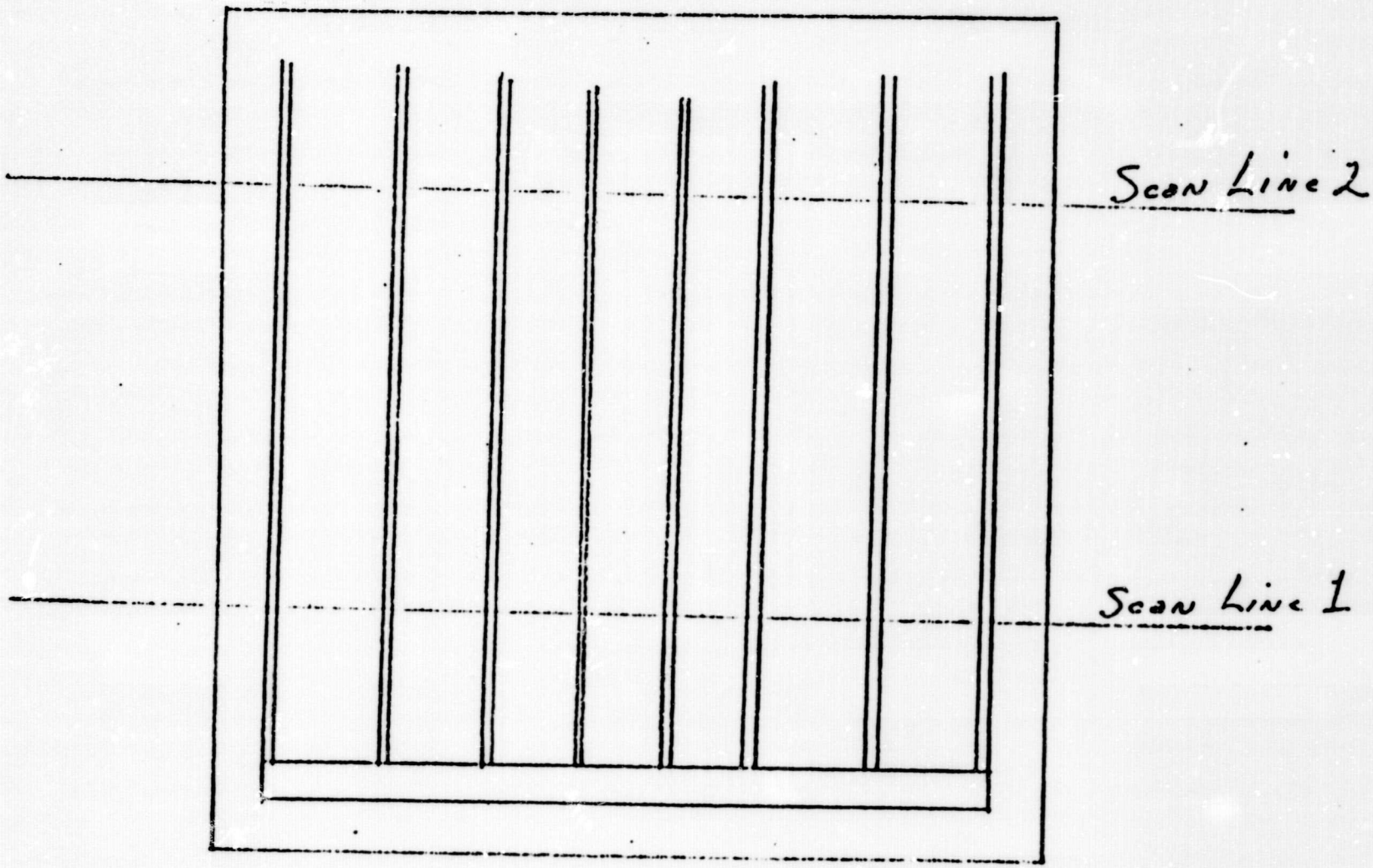

FIG. I

FIG. II-1 Cell # (RTR) 868 c 4 HeNe SCAN

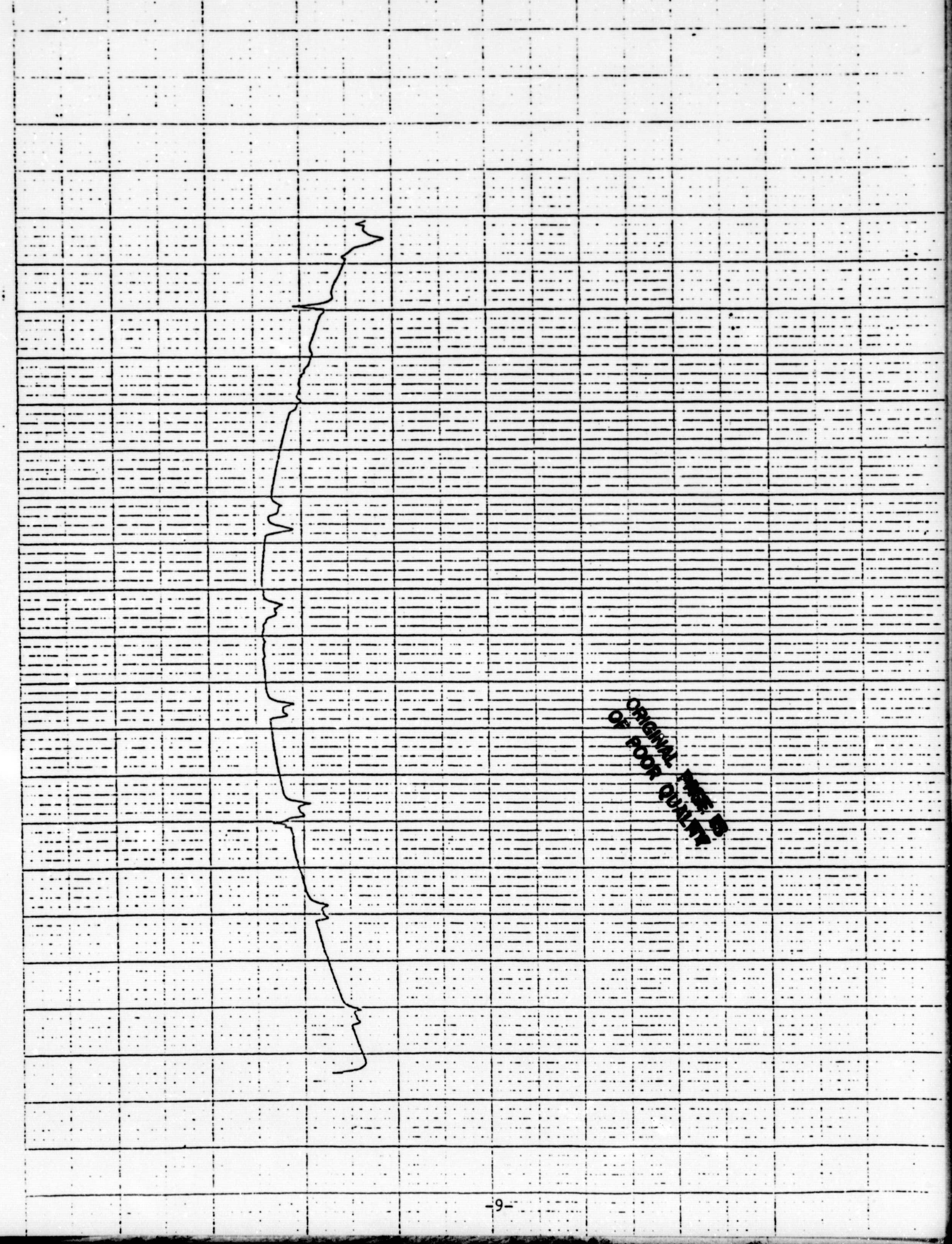

ORIGINAL PAGE IS
OF POOR QUALITY

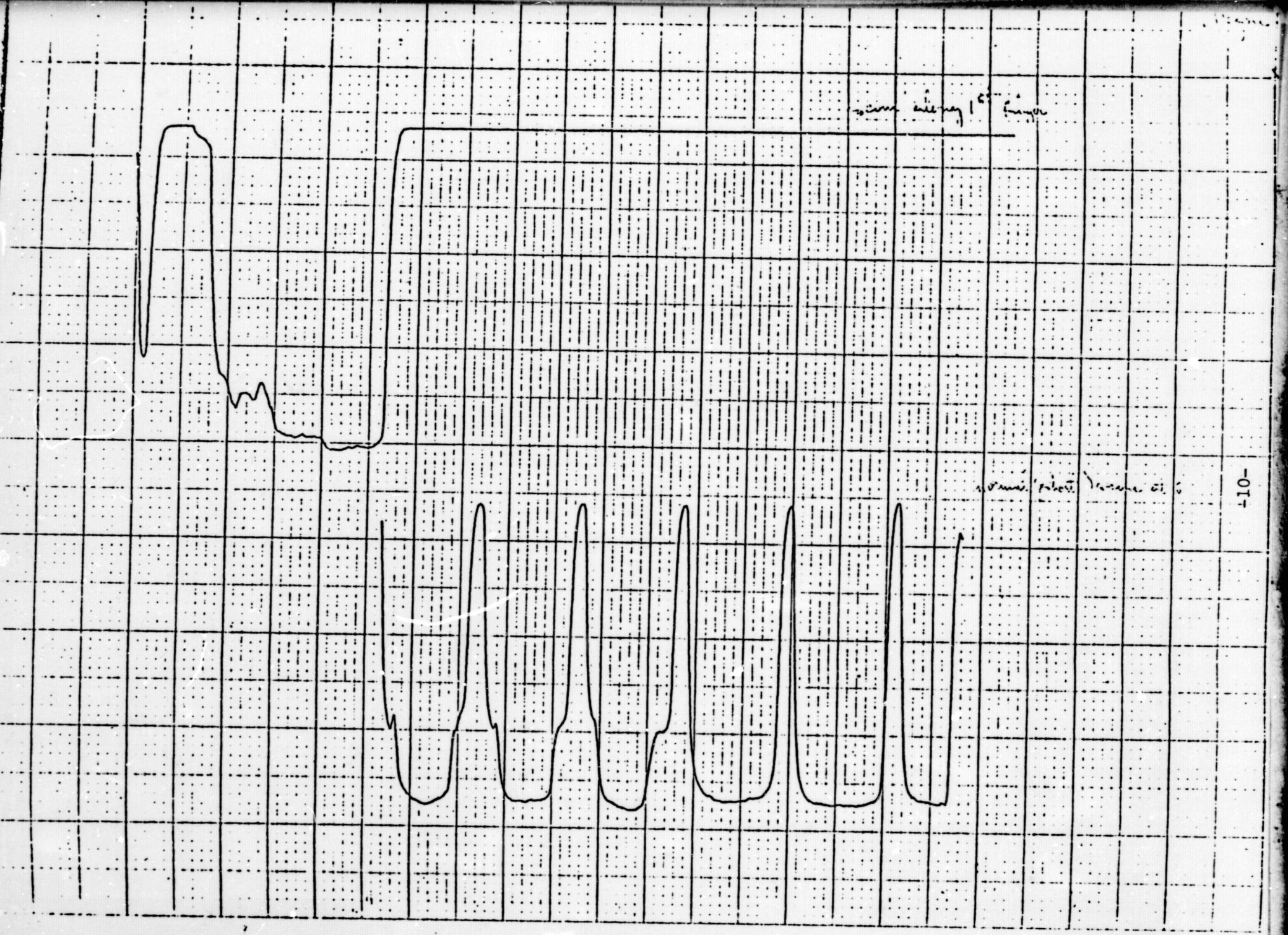

FIG. II-3 CELL 868 C 4 (RTR) ARGON SCAN

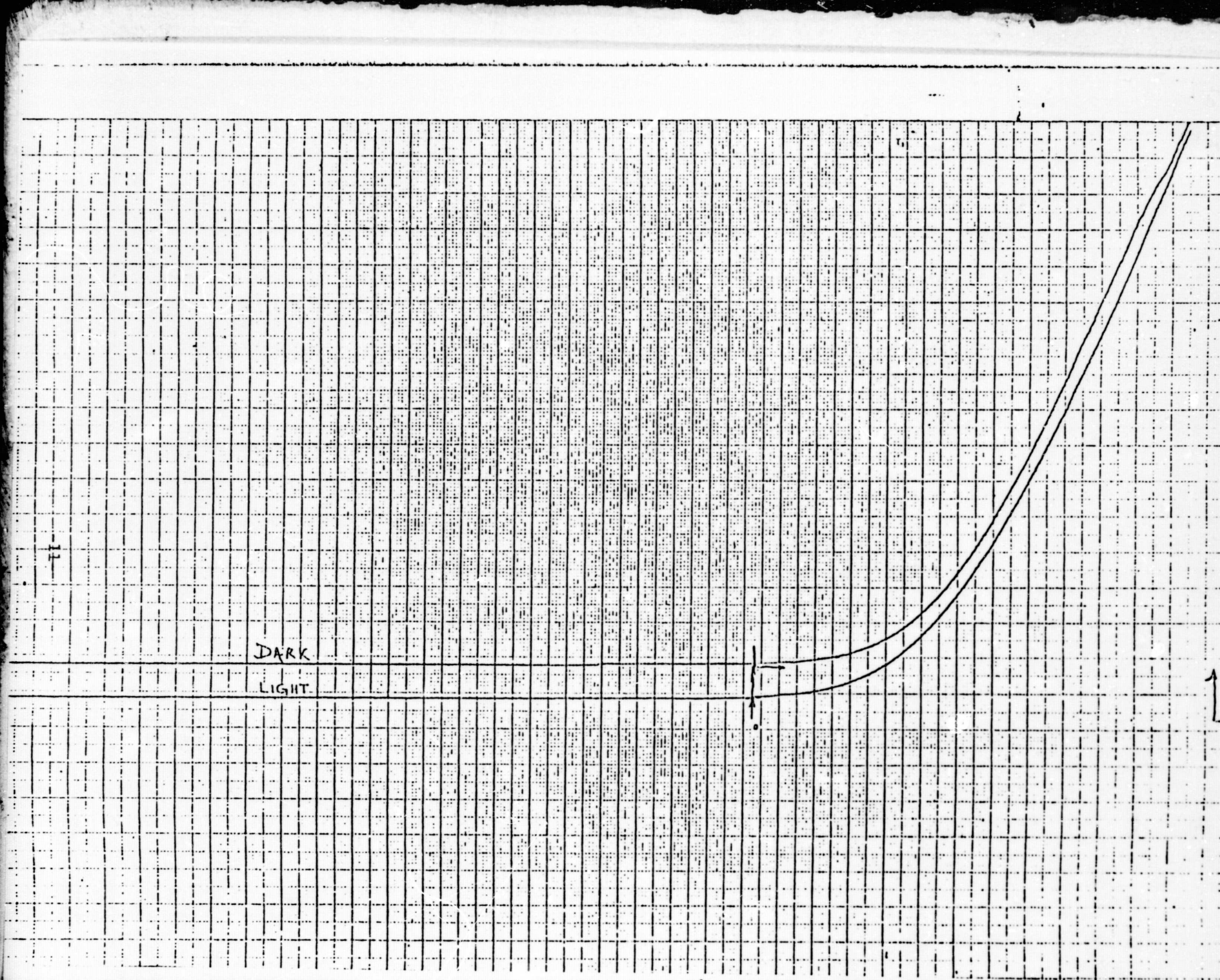
DARK
LIGHT

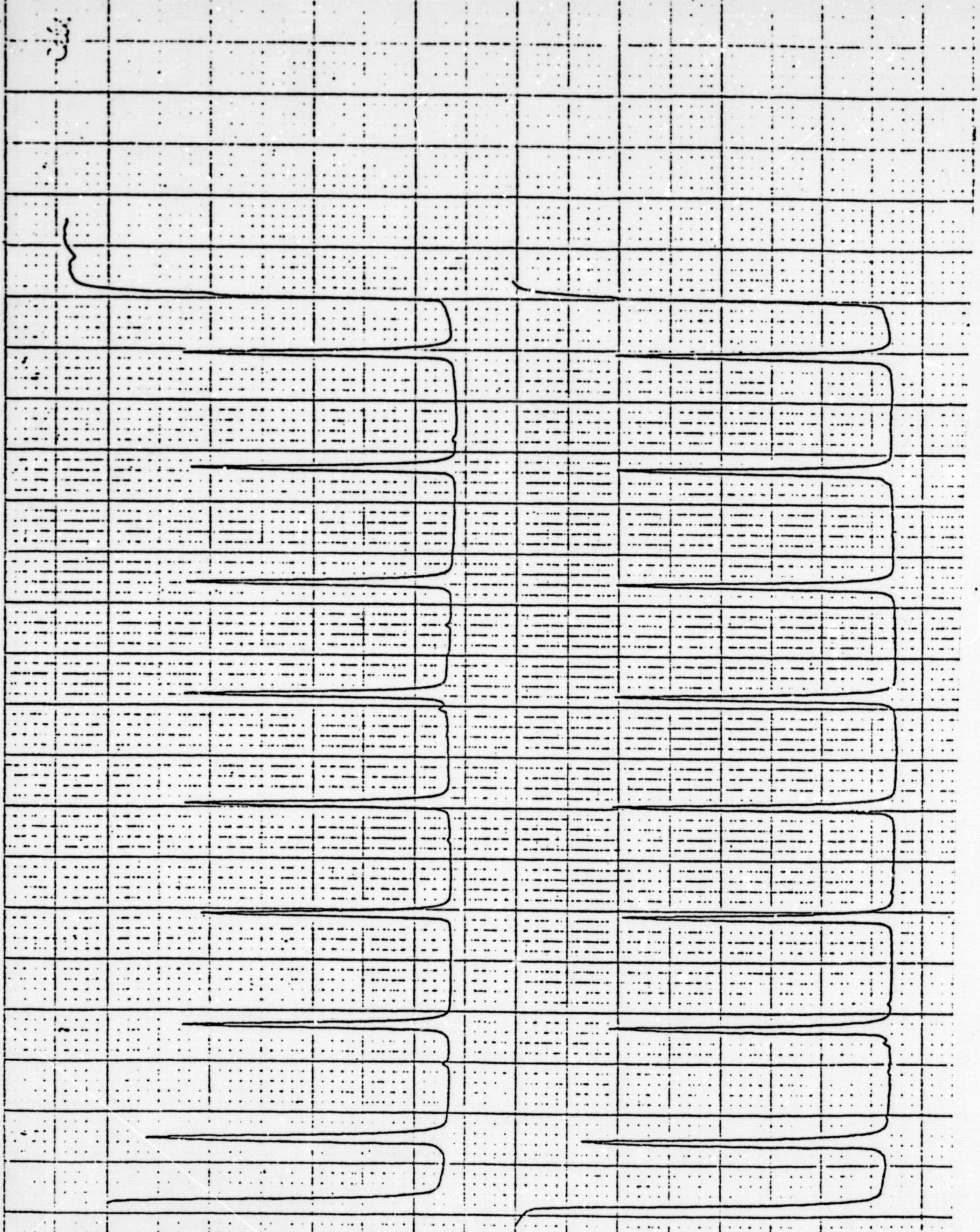

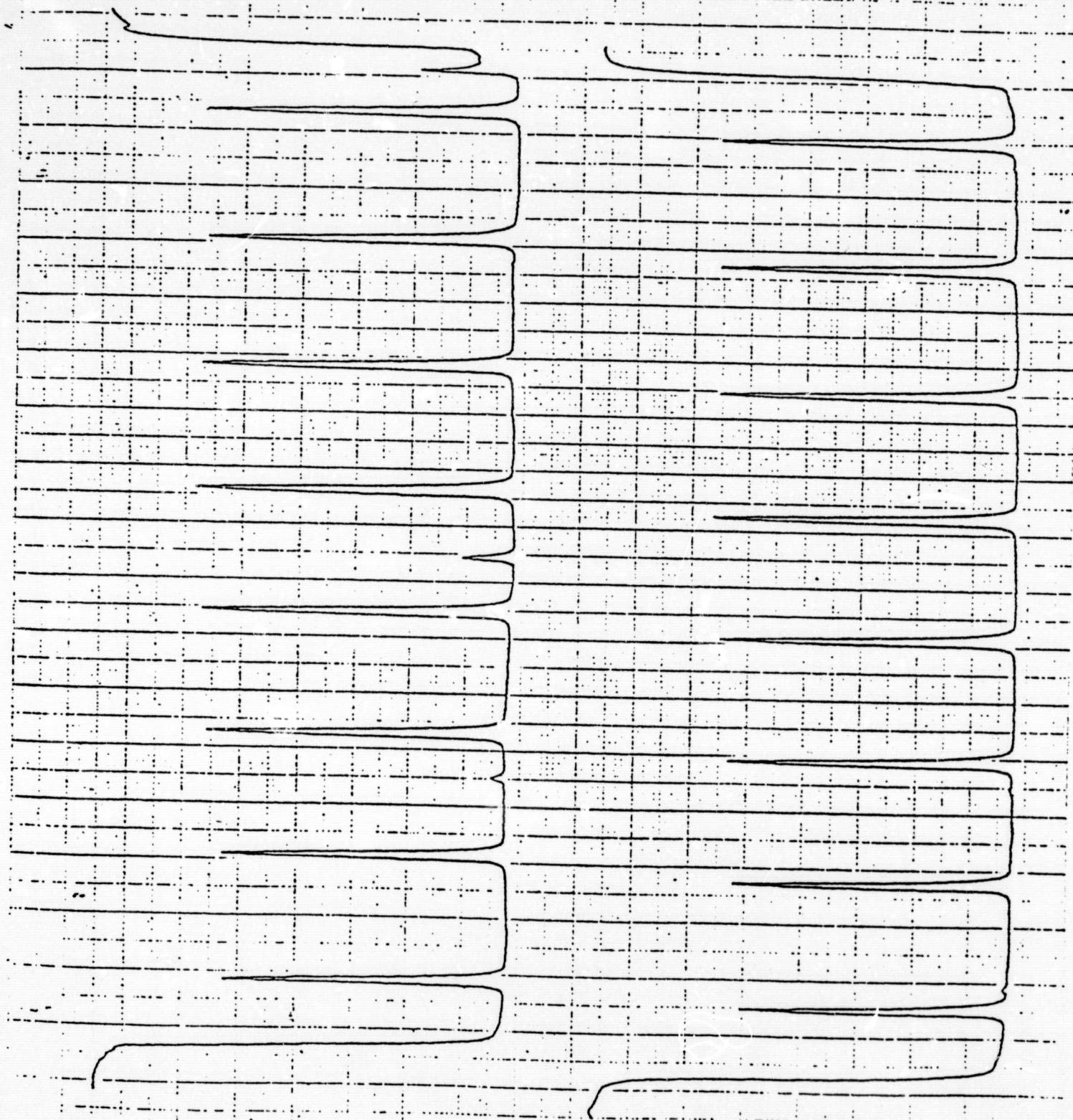

ORIGINAL PAGE IS
OF POOR QUALITY

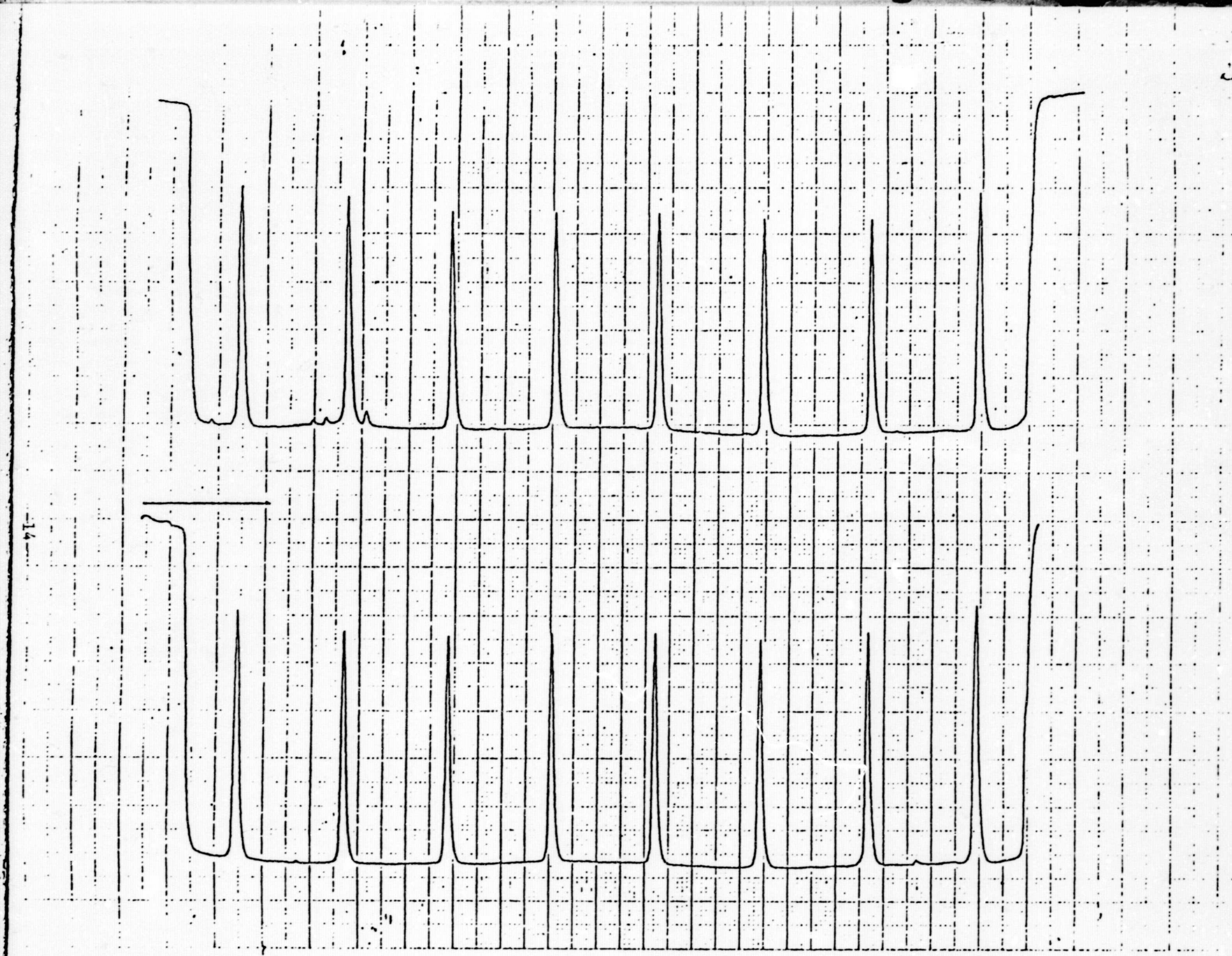

FIG. 5.1 CELL # RE 24-1.5-7° (WEB) HeNe SCAN

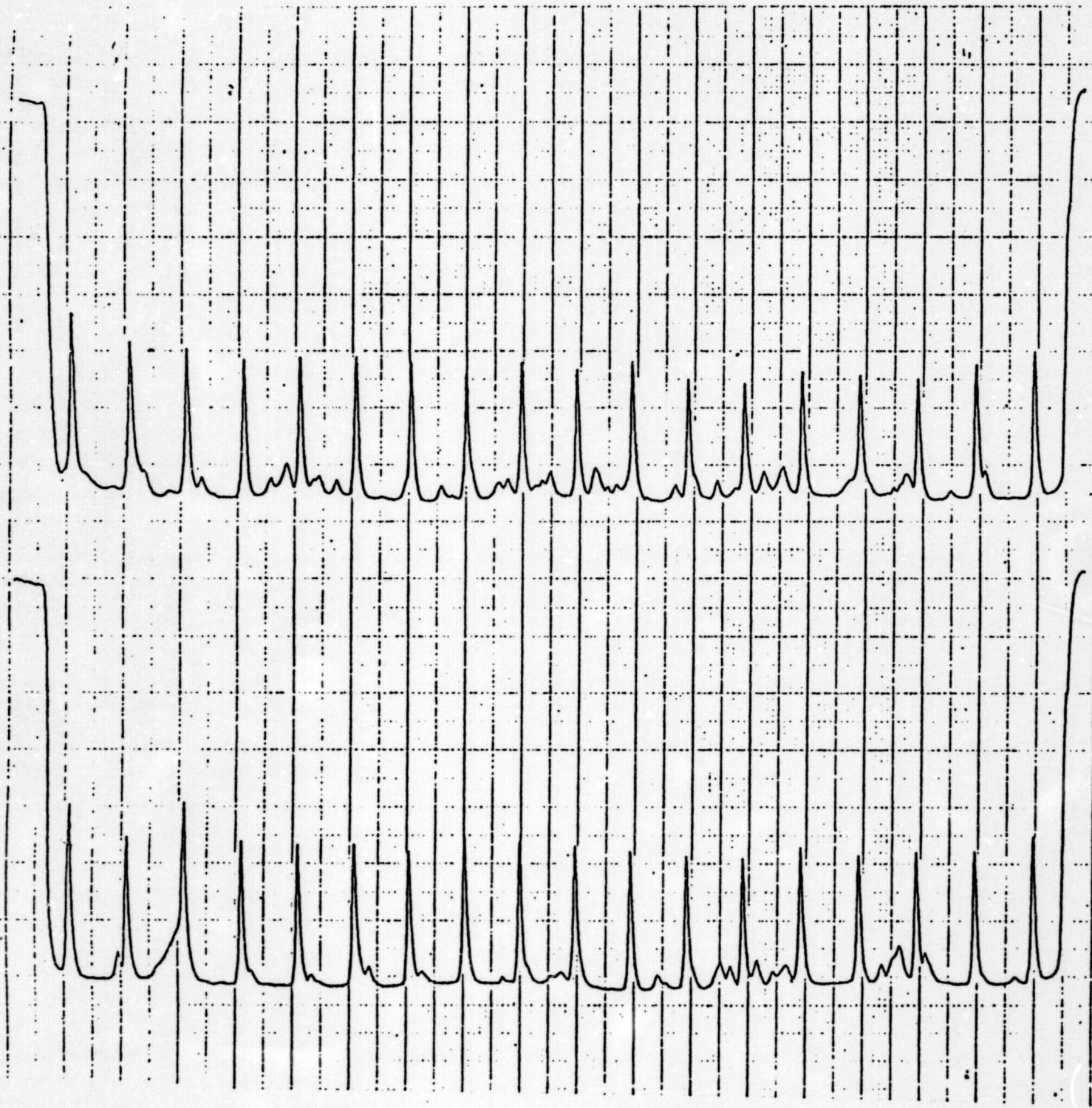

FIG. 6.1 CELL # W-11-3 (WACKER) H_2N_2 SCAN

ORIGINAL PAGE IS
OF POOR QUALITY

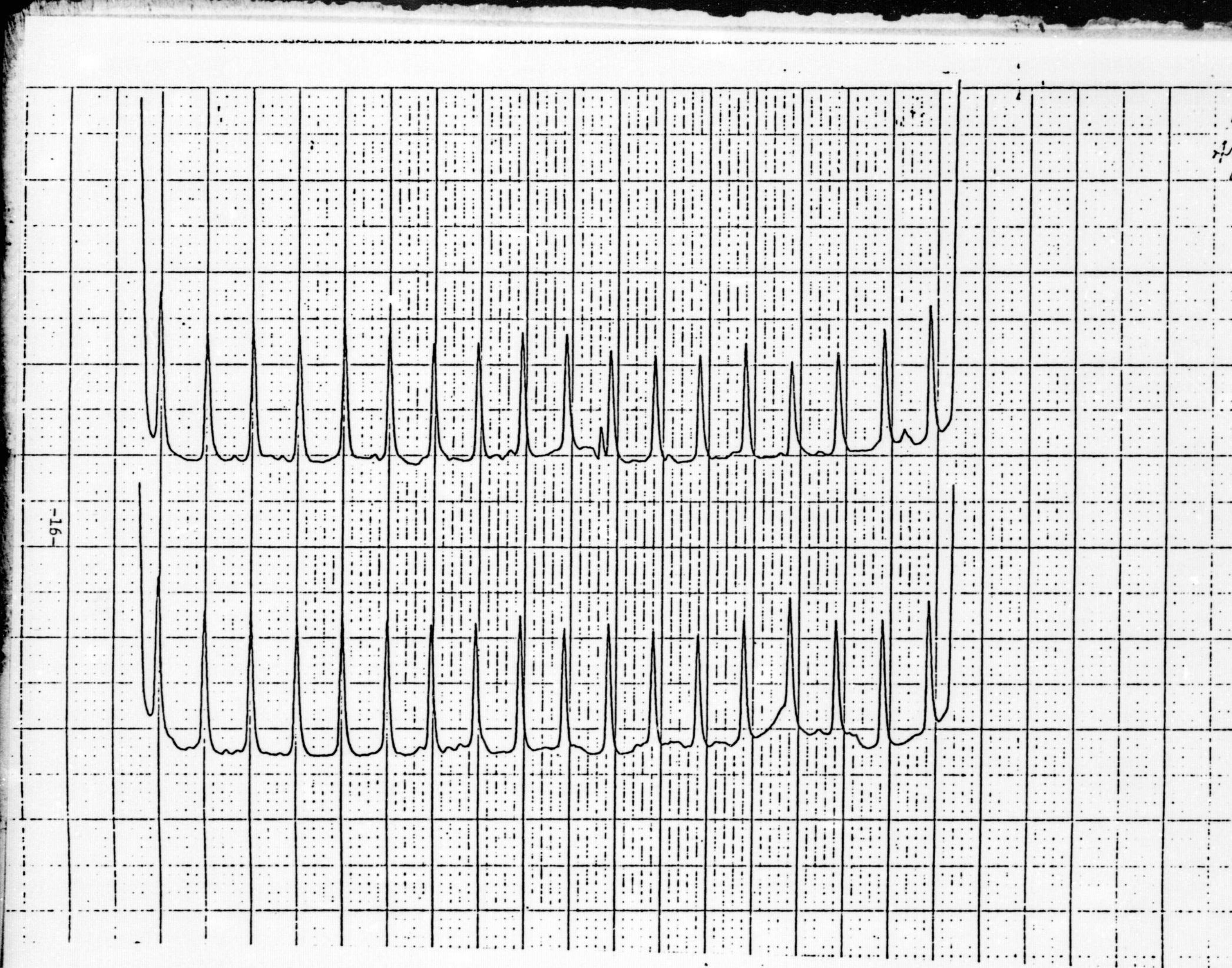

FIG. 6.2 CELL # W-11-3 (WACKER) ARGON SCAN

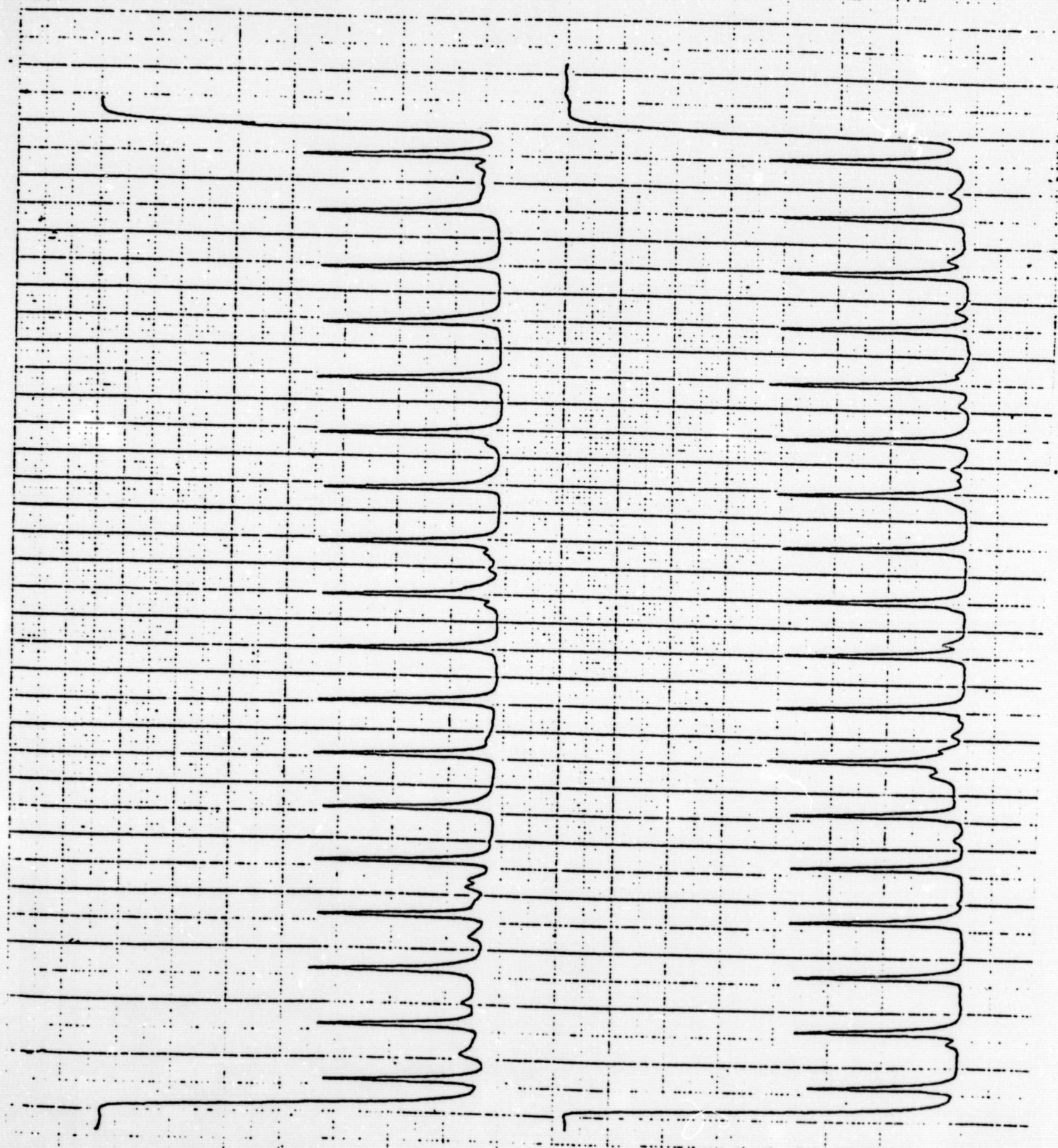

ORIGINAL PAGE IS
OF POOR QUALITY

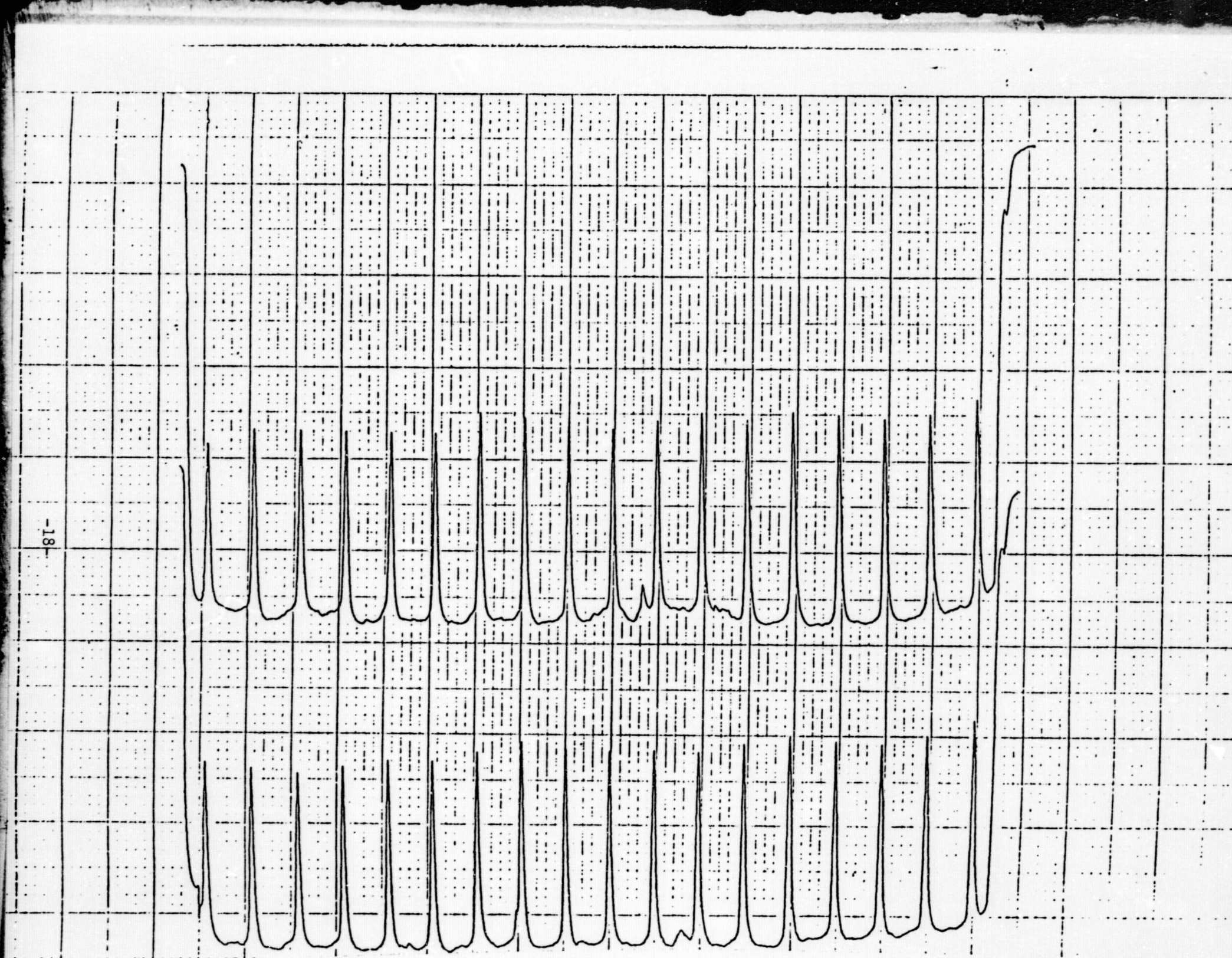

FIG. 7.2 CELL # W-11-17 (WACKER) ARGON SCAN

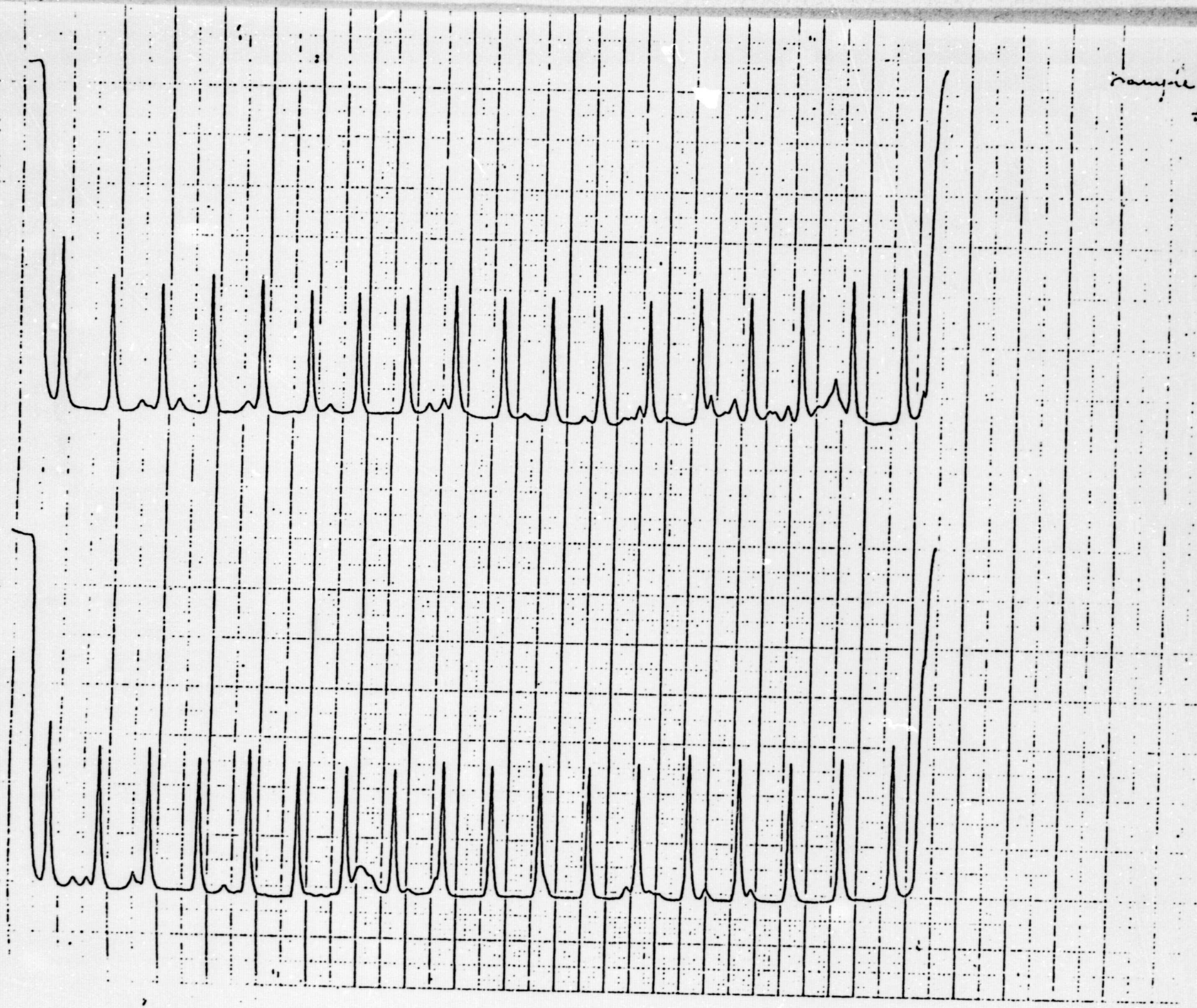

FIG. 8.1 CELL # W-4-4 (WACKER) HeNe SCAN

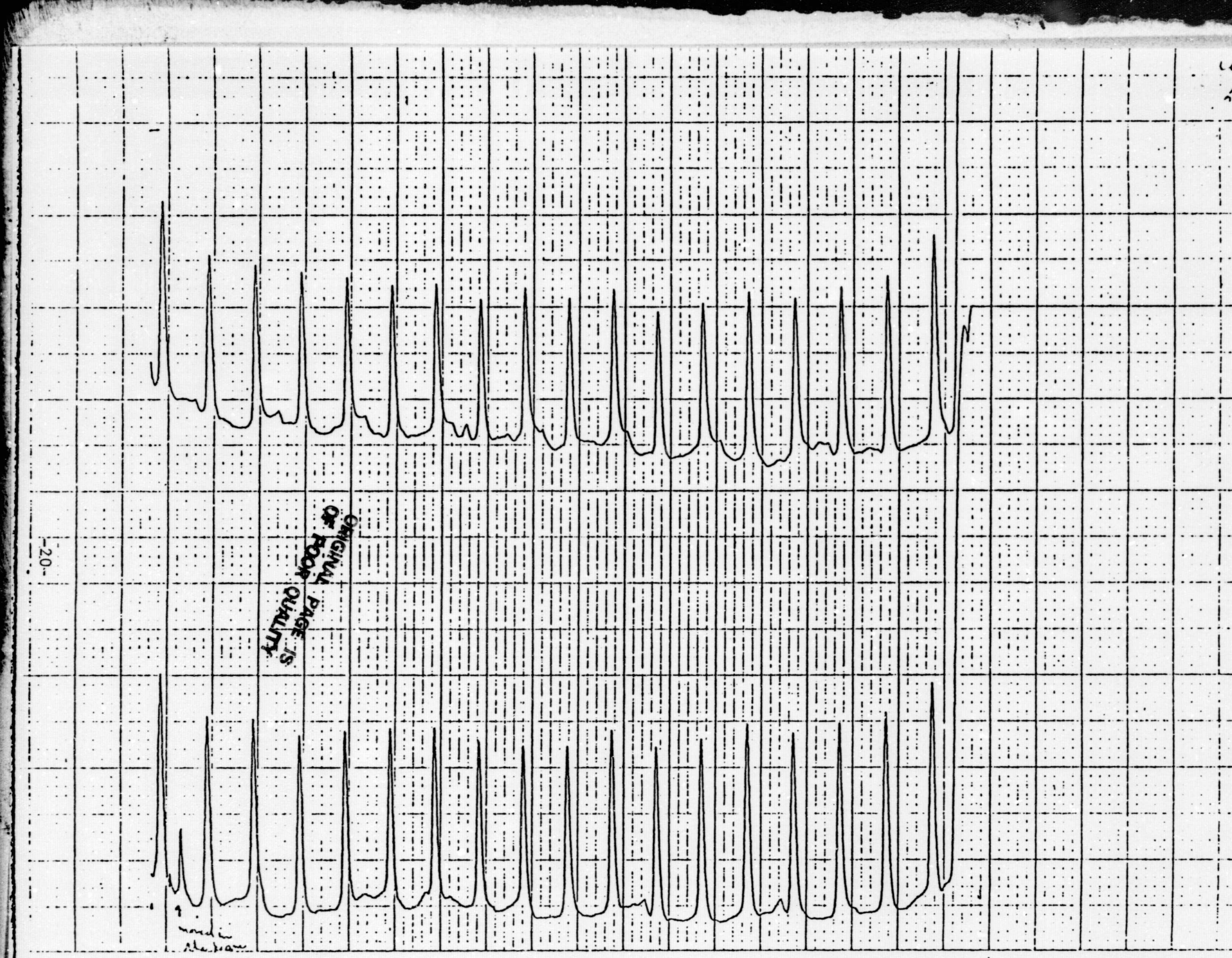

FIG. 8.2 CELL # W-4-4 (WACKER) ARGON SCAN

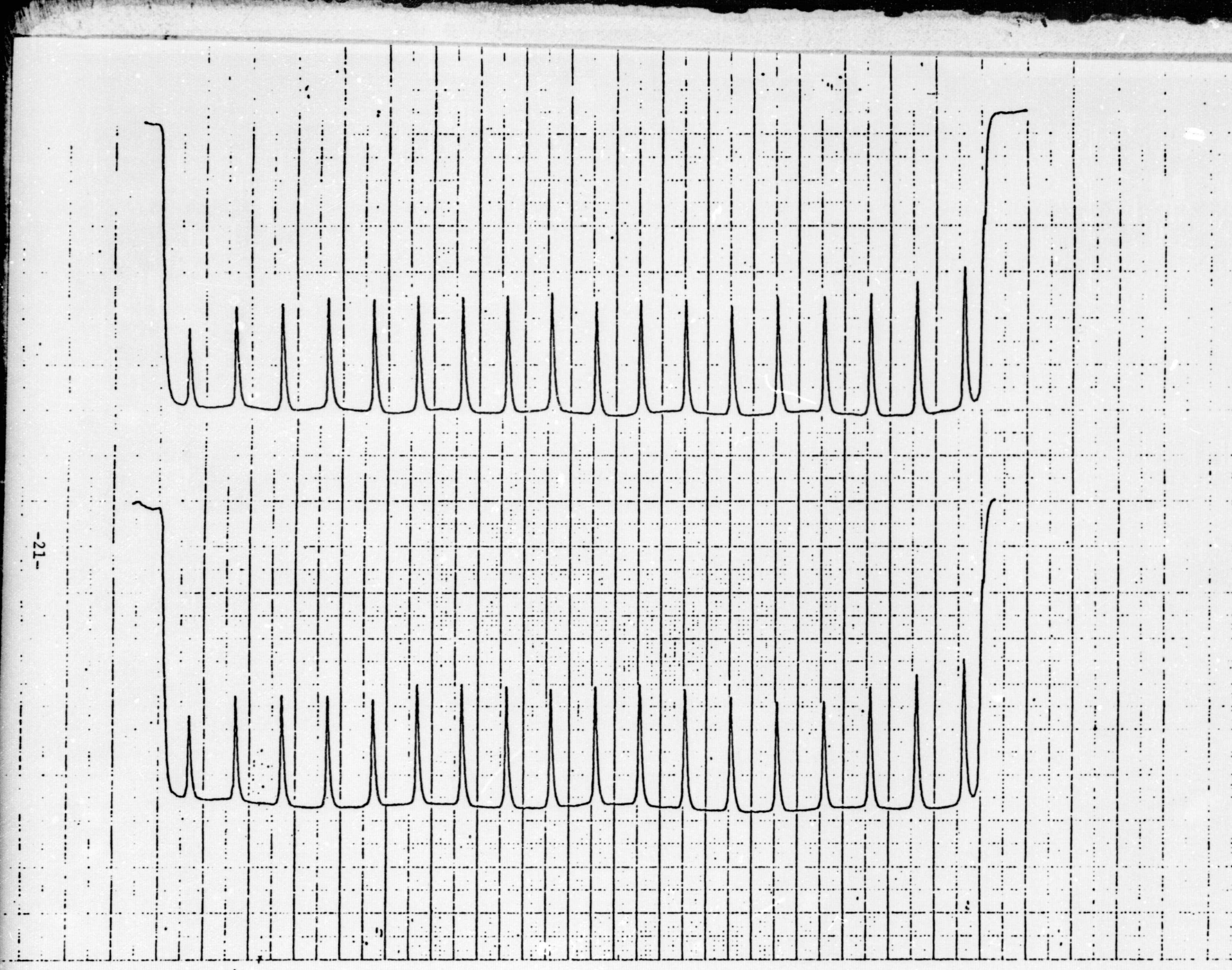

FIG. 9.1 CELL # W-11-8 (WACKER CONTROL) HeNe SCAN

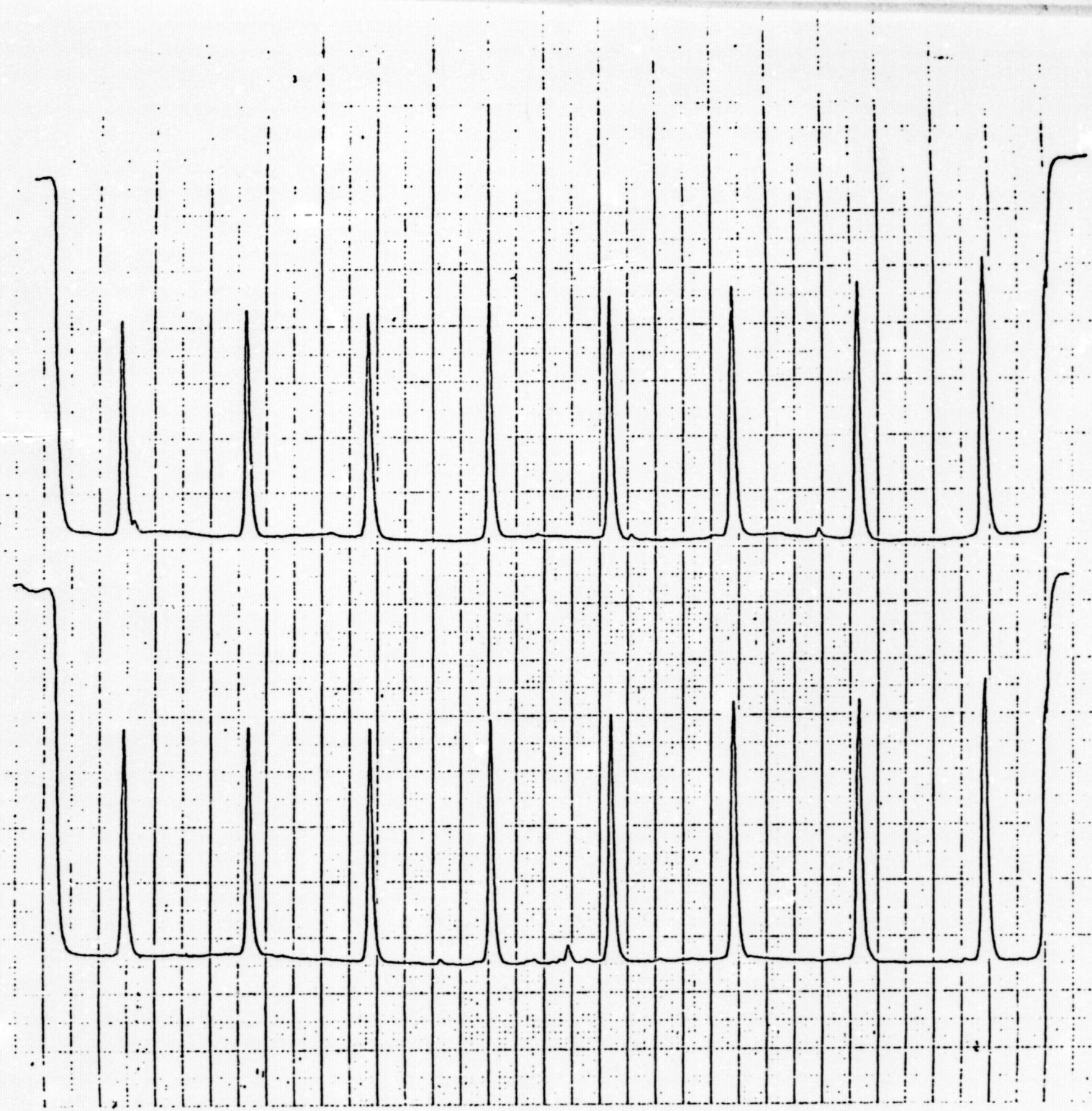

FIG. 10-1 CELL # 1-852-52 (CSI) HeNe SCAN

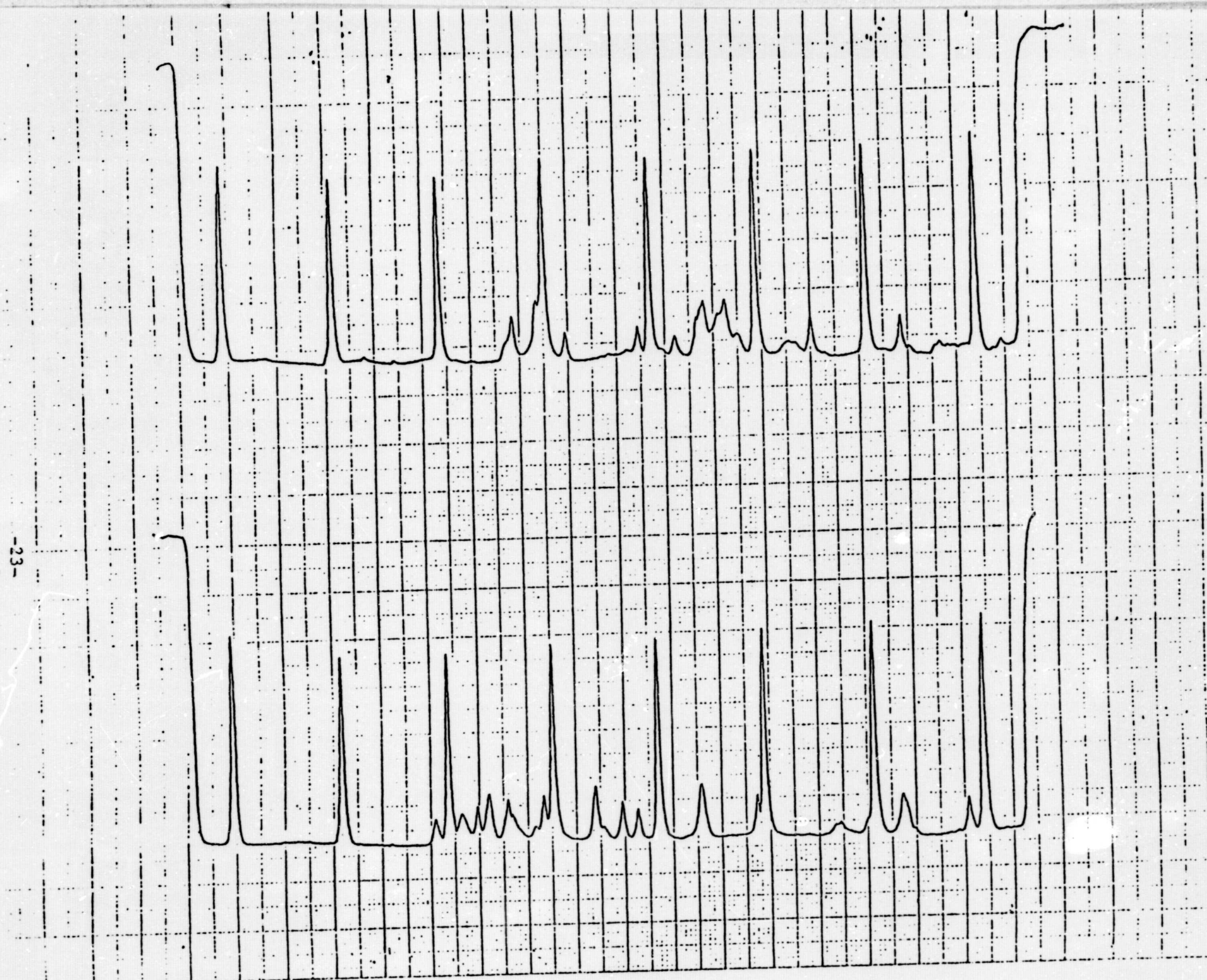

FIG. 11.1 CELL # 1-860-46 (CSI) HeNe SCAN

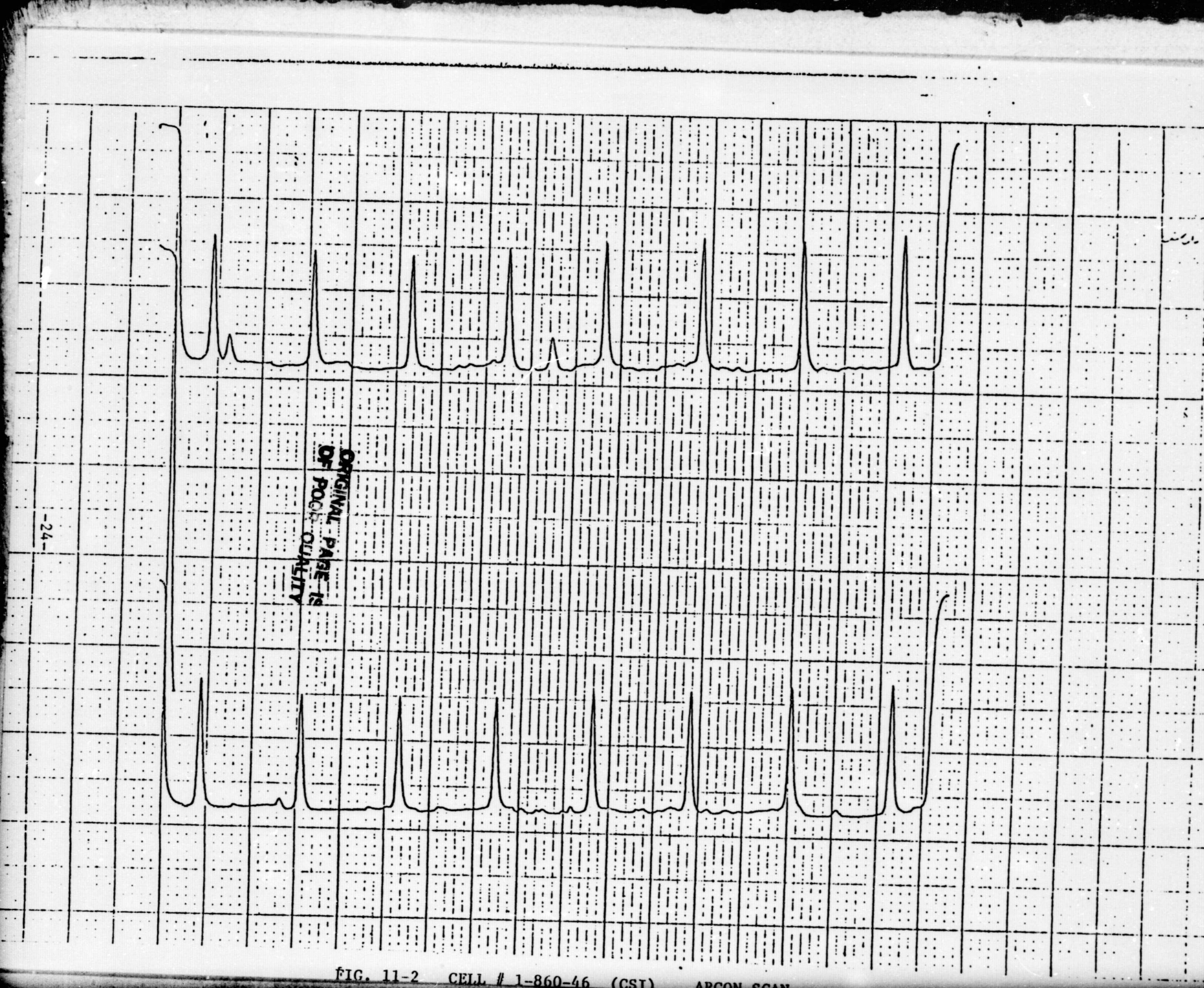

FIG. 11-2 CELL # 1-860-46 (CSI) ARGON SCAN

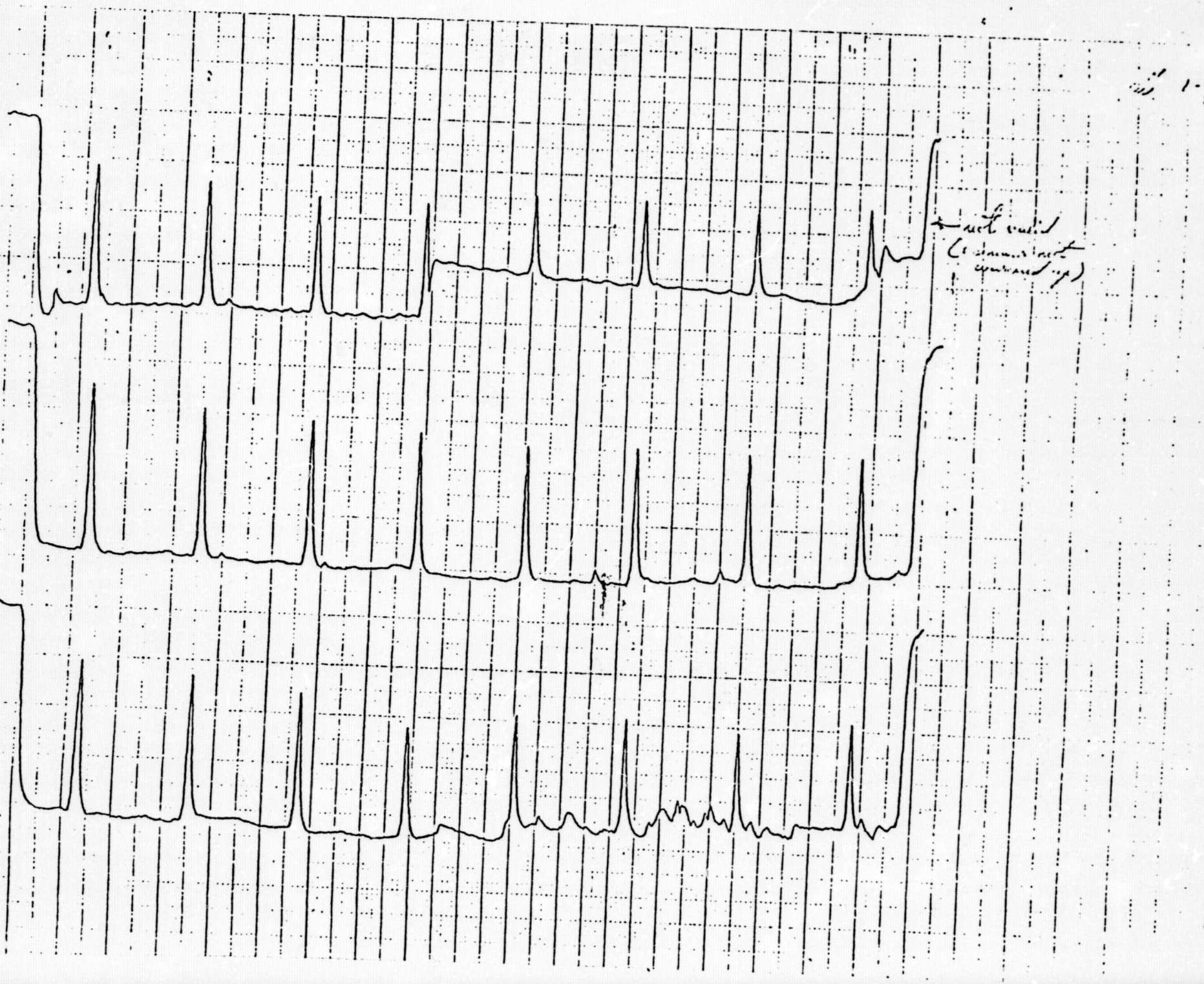

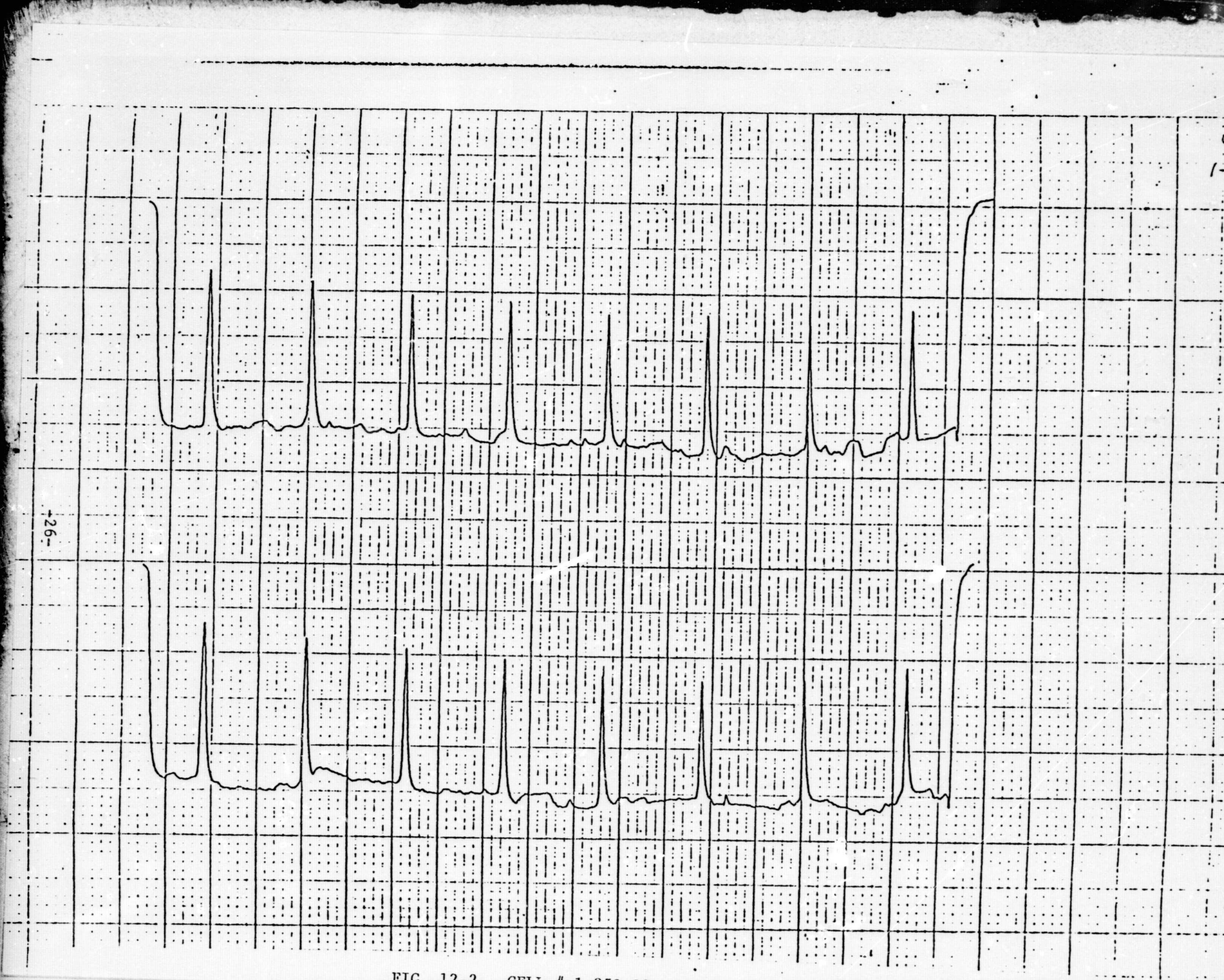

FIG. 12-2 CELL # 1-852-23 (CSI) ARGON SCAN

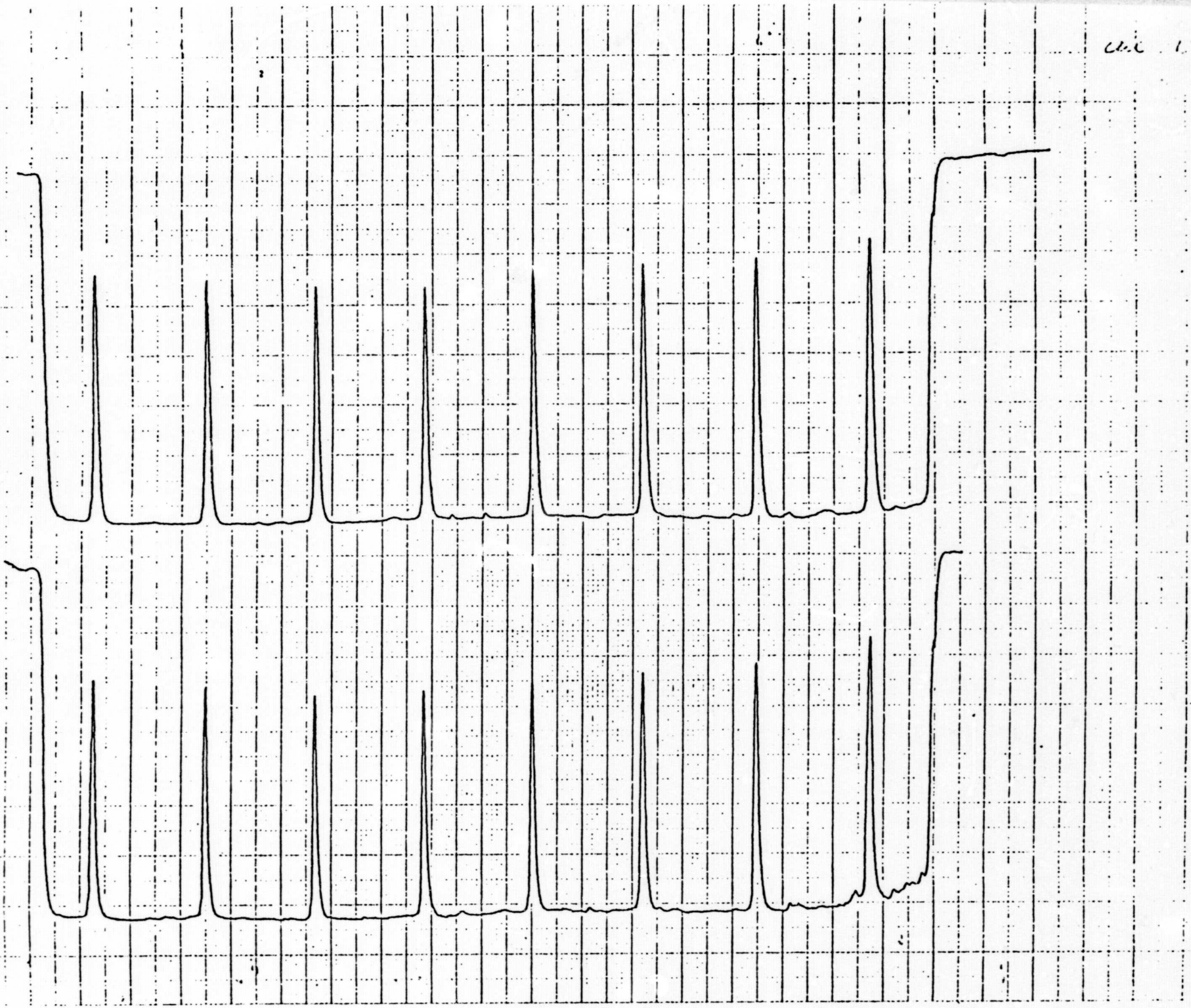

FIG. 13.1 CELL # 1-852-41 (CSI) HeNe SCAN

ORIGINAL PAGE IS
OF POOR QUALITY

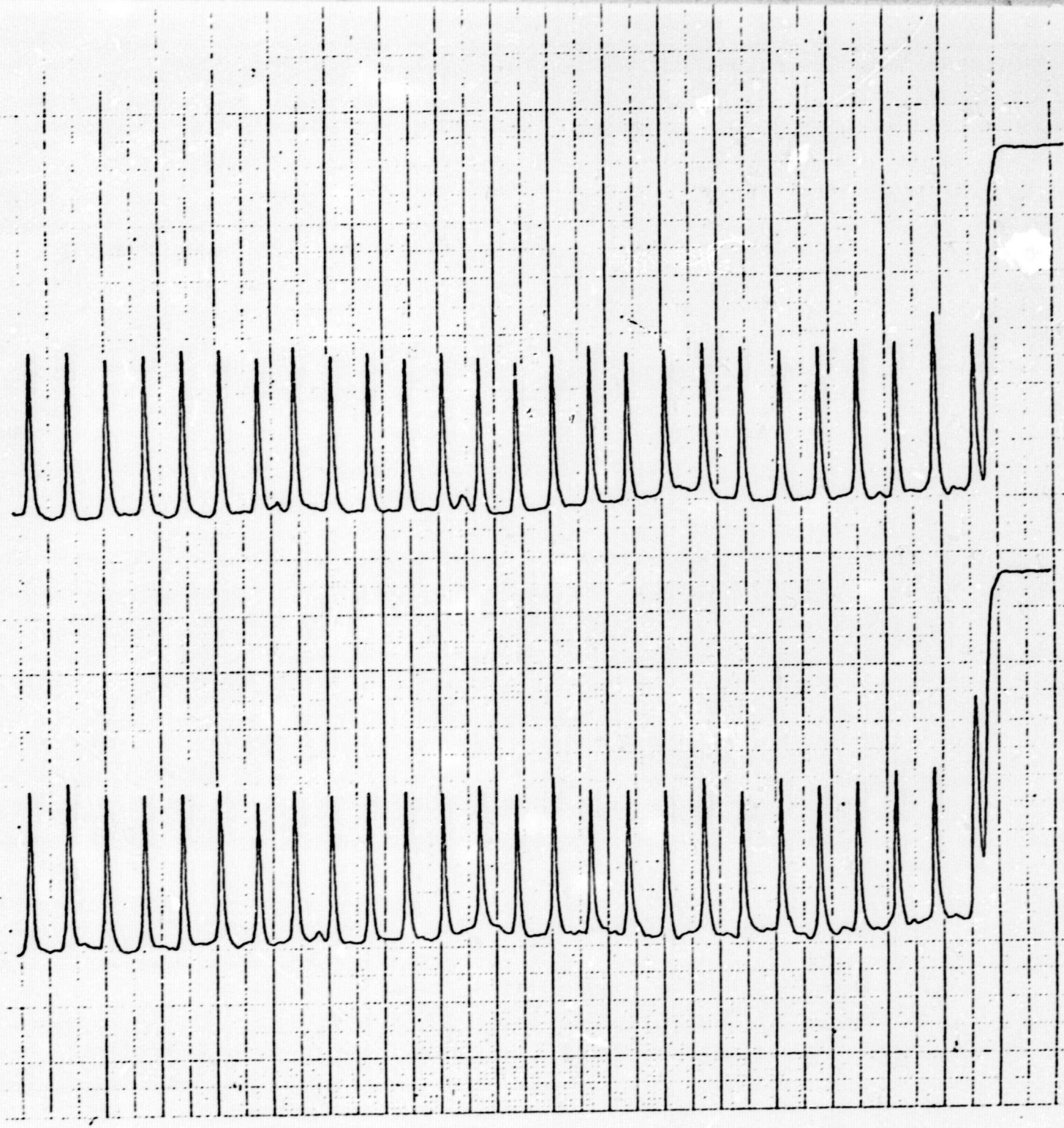

FIG. 14.1 CELL #8 (EFG) HeNe SCAN

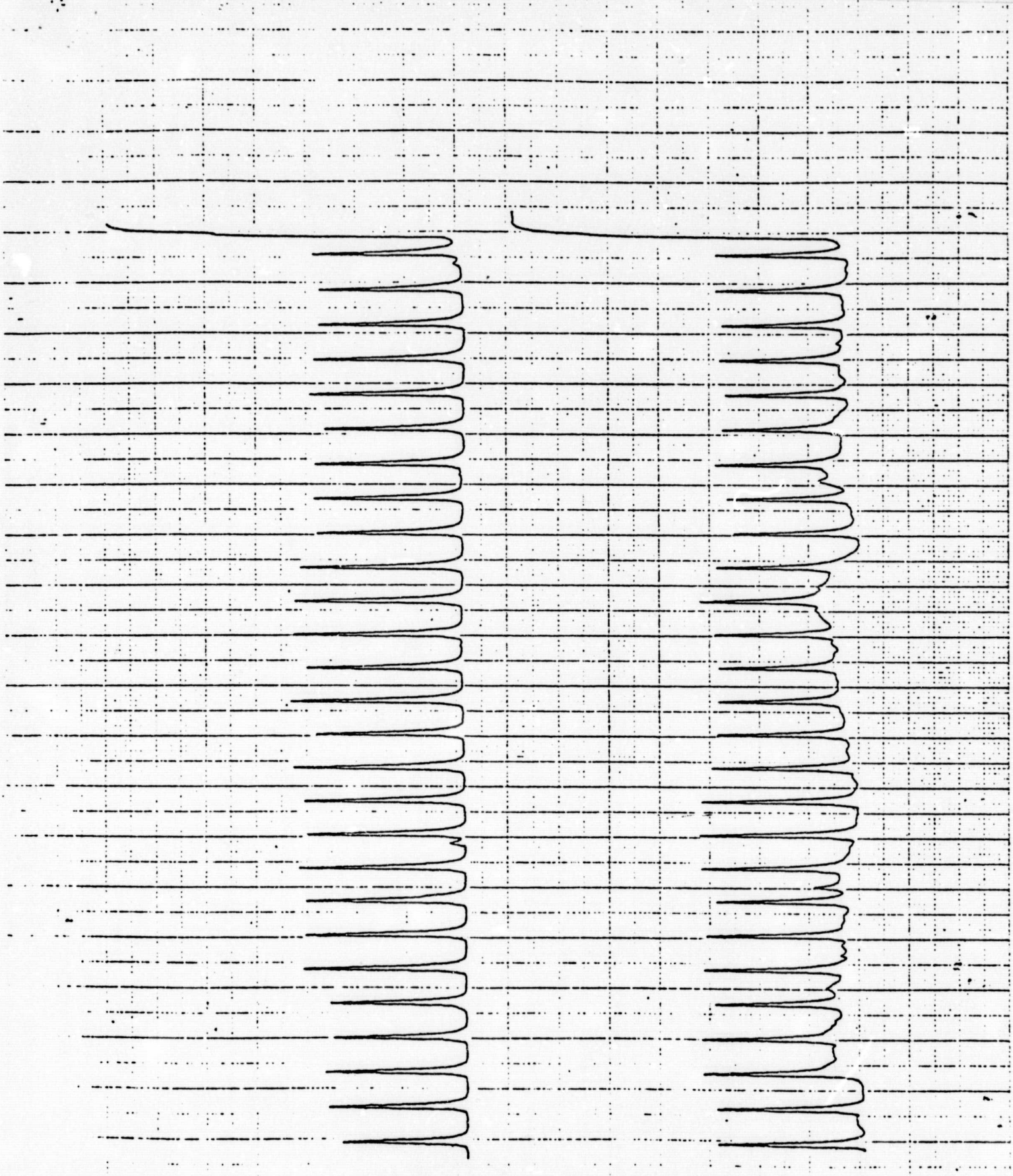

FIG. 15-1 CELL # 28 (EFG) HeNe SCAN

ORIGINAL PAGE IS
OF POOR QUALITY

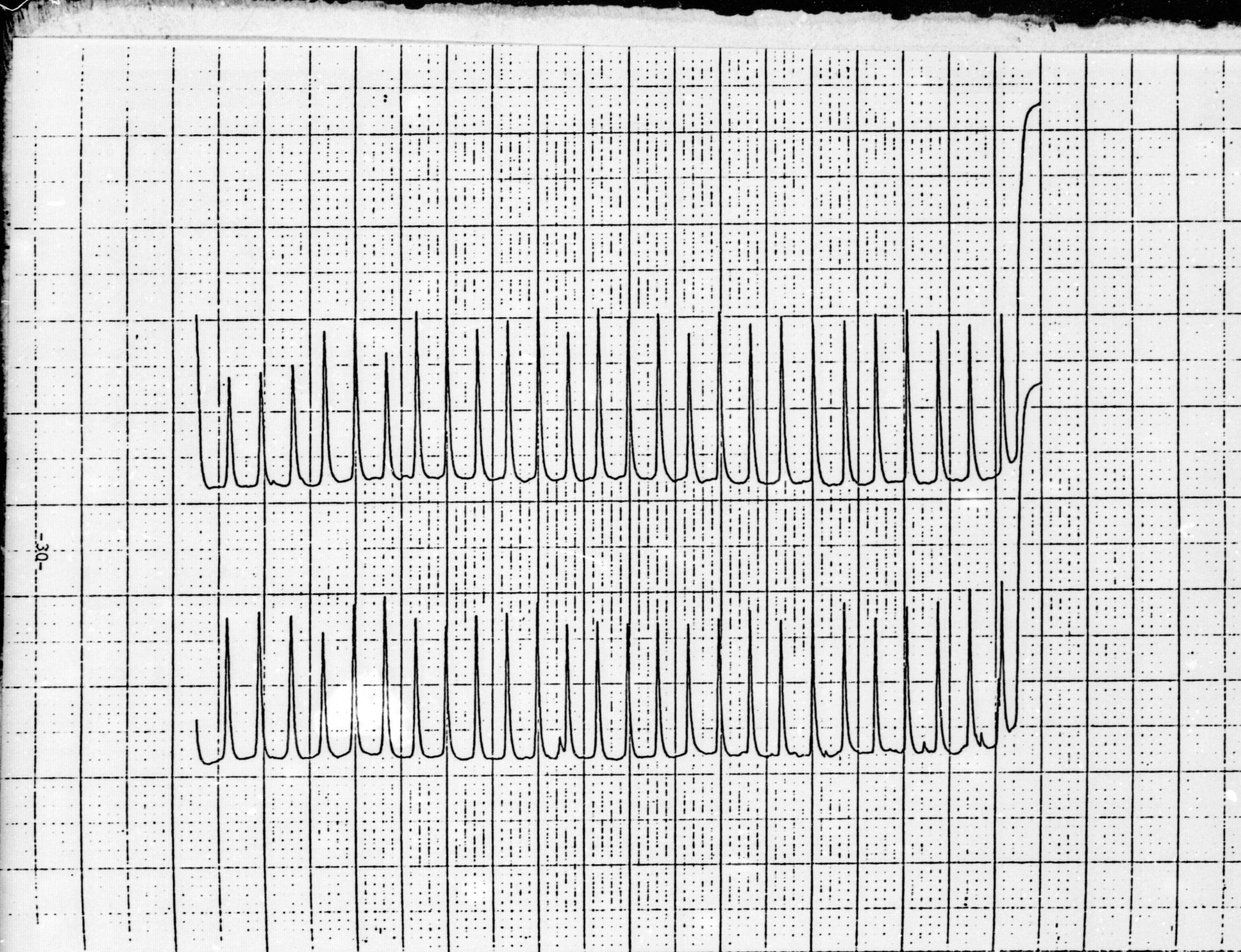

FIG. 15.2 CELL # 28 (EFG) ARGON SCAN

FIG. 16.1 CELL # 36 (EFG) He-Ne SCAN

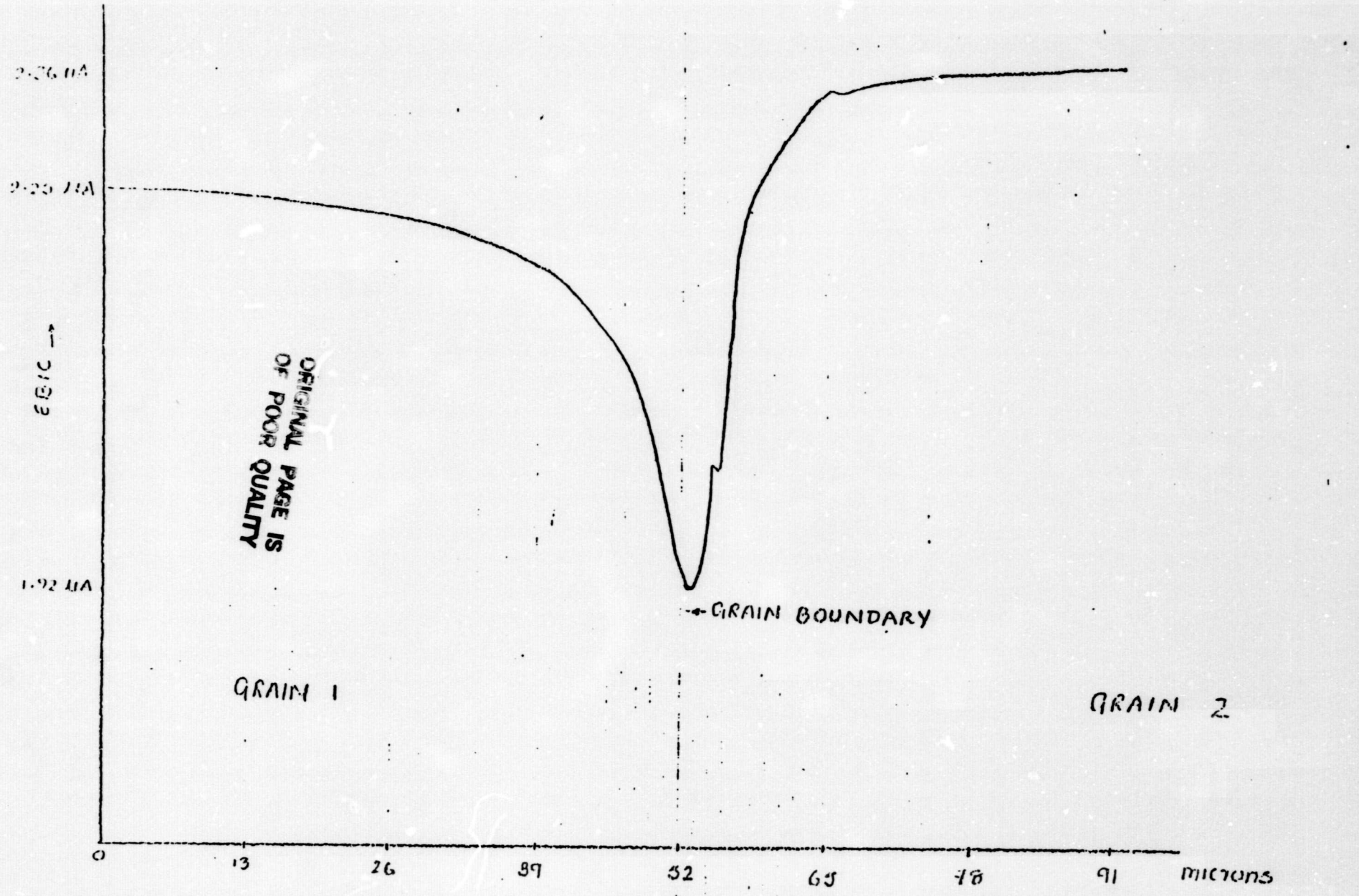

ORIGINAL PAGE IS OF POOR QUALITY

Figure 19 experimental EBIC near a grain boundary

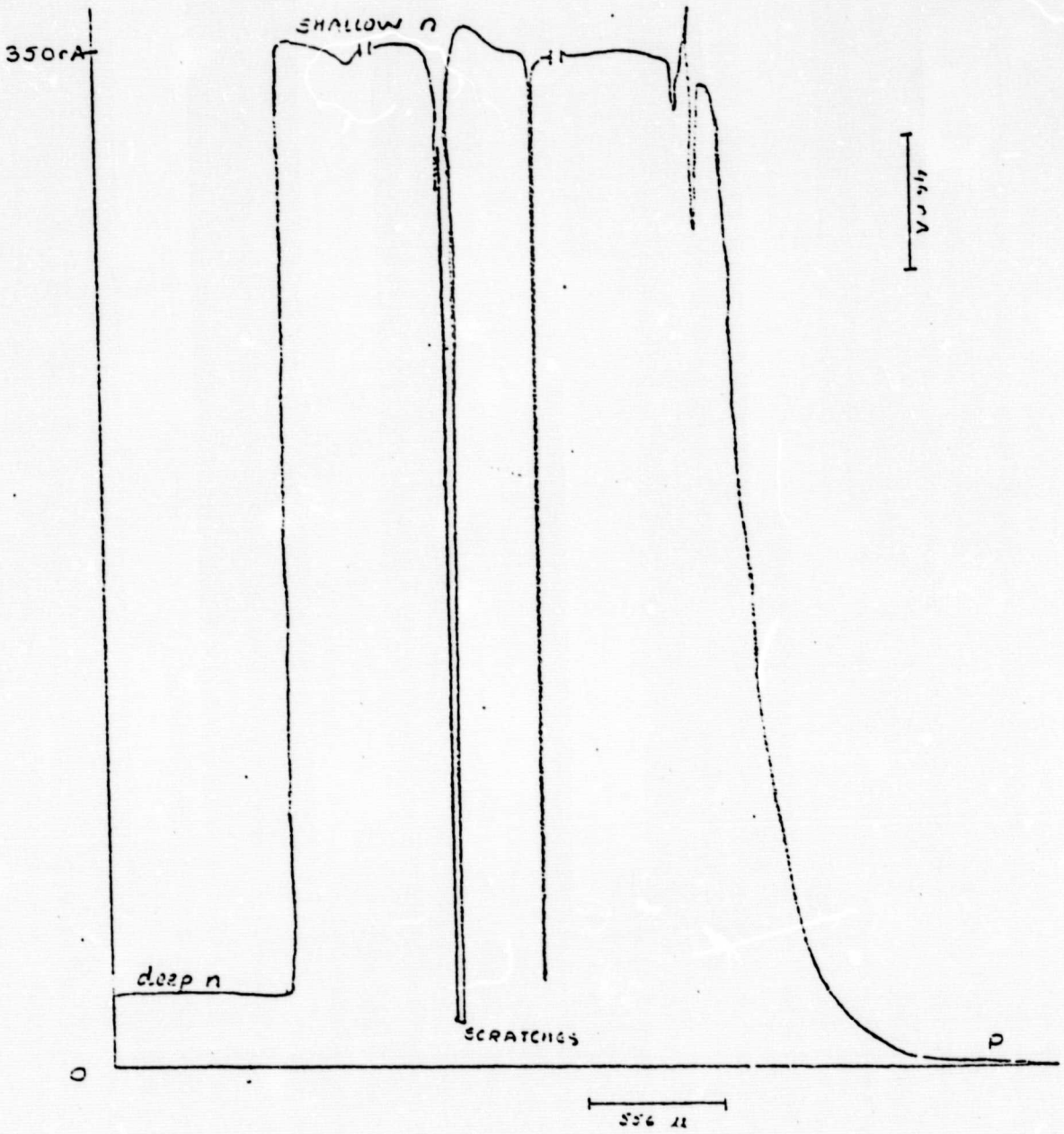

Figure 18 Experimental EBIC near a grain boundary

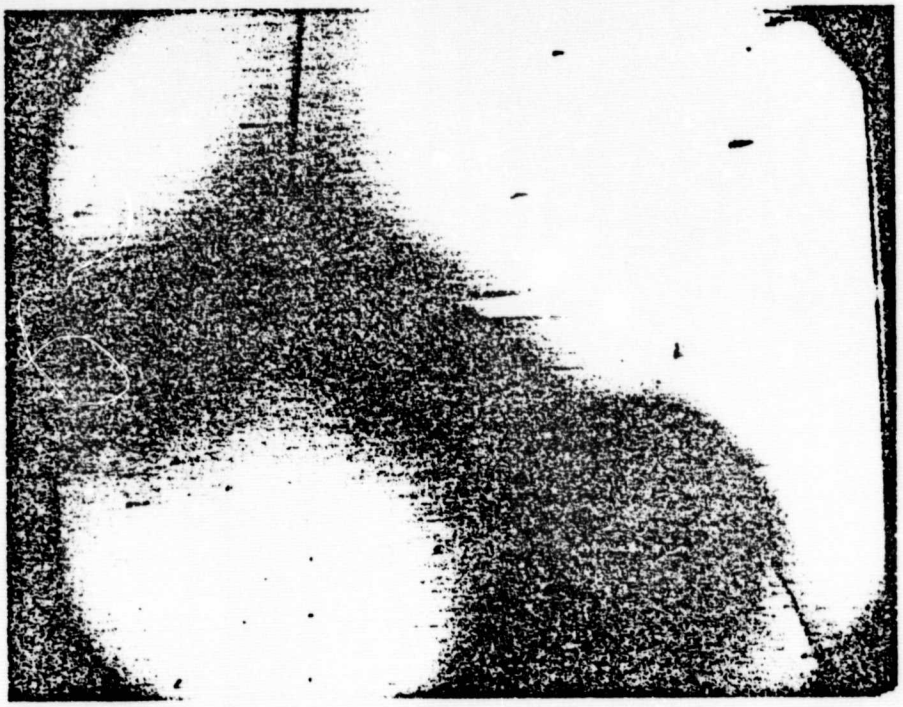

ORIGINAL PAGE IS
OF POOR QUALITY

Fig. 17 - EGIC pictures of deep (light and shallow portions of a p-n junction.
Magnification: x20
Beam Voltage: 19 KN.